

Impurity states and interlayer tunneling in high temperature superconductors

I. Martin¹, A.V. Balatsky¹, and J. Zaanen²

¹ Theoretical Division, Los Alamos National Laboratory, Los Alamos, NM 87545,

² Physics Department, Leiden University, The Netherlands

(Printed December 2, 2024)

We argue that the Scanning Tunneling Microscope (STM) images of impurity states generated by doping Zn or Ni impurities into Cu-O plane of BSCCO are the result of quantum interference of the impurity signal coming from several distinct paths. An impurity image seen on the surface is greatly affected by interlayer tunneling matrix elements. We find that the easiest tunneling path for an STM electron is to tunnel through the Bi 4s orbital into the Zn or Cu 4s orbital and only then into the Cu $d_{x^2-y^2}$ orbitals in the plane. This tunneling path leads to the four-fold nonlocal filter of the impurity state in Cu-O plane. The tunneling of carriers occurs in a manner similar to the interlayer tunneling in the pure system. We point out that the filter depends on the particular compound and can be different for YBCO.

Recently S.H. Pan and collaborators applied the STM technique to image single Zn and Ni impurities in optimally doped BSCCO [1,2]. These experiments proved that one can image single impurity states in an unconventional superconductor and demonstrated the highly anisotropic structure of these states.

Although it appears that on a gross scale these findings can be understood in terms of a conventional d -wave superconductor perturbed by potential scattering, upon closer inspection problems of principle seem to arise. The impurity states observed by STM are characterized by two main features: (1) energy and width of the impurity induced peak in the density of states (DOS), and (2) the spatial structure of the impurity induced resonance. While the DOS seems to be satisfactorily described by a simple one site potential and magnetic interaction, the real space distribution of intensity cannot be fit by a simple impurity model [3]. The main problem with the Zn impurity image, as seen in the STM experiments, is that the intensity of the signal on the impurity site is very bright, which is at odds with the unitary scattering off Zn. We remind that Zn^{2+} has a closed d shell and hence, exactly on the impurity site the scattering potential is very strong. Unitary scattering is equivalent to the hard wall condition for the conduction states and therefore *no or very little intensity* of electron states is expected on the Zn site.

Here we demonstrate that these problems find a natural resolution in terms of the specific way in which the local density of states of the cuprate planes is probed in the STM experiments. We argue that the quantum mechanical nature of the tunneling from the STM tip into the Cu-O layer that hosts impurity requires tunneling through the uppermost insulating Bi-O layer which effectively filters the signal. This tunneling has profound consequences for the real space image of the impurity state seen by STM. Tunneling between Bi-O and Cu-O layers occurs via 4s orbitals of Bi and Cu or Zn [4,5]. As a result, the electron/hole arriving in the Cu-O plane is

in s -wave state and hybridizes with the *neighboring* Cu sites via the d -wave like matrix element $M_{i,j}$:

$$M_{i,j} \sim \Psi_{i+1,j} + \Psi_{i-1,j} - \Psi_{i,j+1} - \Psi_{i,j-1} \quad (1)$$

where $\Psi_{i,j}$ is the impurity state wavefunction on site (i,j) . The tunneling matrix element determines the intensity of the impurity signal $F[\Psi_{i,j}] = |M_{i,j}|^2$. We call this effect *filtering*. The filtering effect induces the d -wave-like *fork* which samples the impurity state (see Fig. 1).

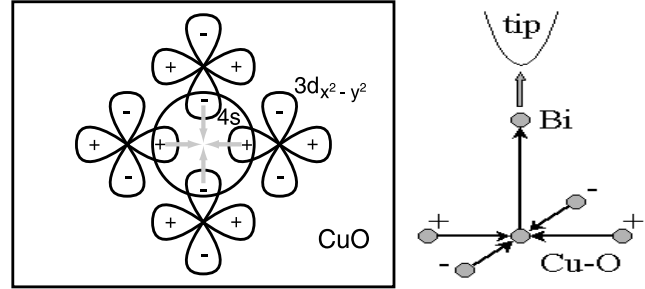


FIG. 1. Tunneling from Cu-O layer into Bi-O layer occurs through the empty high-energy 4s Cu and Bi orbitals. Tunneling into a particular Bi atom effectively probes four Cu $d_{x^2-y^2}$ orbitals with the signs of the contributions given by the overlap of these orbitals with the 4s orbital of the atom immediately under the probed Bi atom. This induces a filtering effect which samples the impurity state with the d -wave-like *fork*.

Calculating the local densities of states in the vicinity of the impurity using this filtering function reproduces the features seen in the experiments in great detail (Figs. 3 and 4). The aforementioned anomalies all find an explanation in terms of interferences associated with the non-local way in which the electronic states are probed.

Similar to the Zn case, the Ni impurity tunneling intensity is maximal at the Bi position immediately above the

impurity site. However, there are several important differences between the observed Zn- and Ni-induced states: (1) The energy of the Zn state is close to the chemical potential, $\varepsilon_{\text{Zn}} = -2$ mV, while the Ni state energy is larger and is split, $\varepsilon_{\text{Ni}} = 9$ and 18 mV, (2) the Zn state appears only on the negative bias, while the Ni state shows up both on positive bias and the symmetric negative bias. In this letter we demonstrate how all of these experimental features can be obtained within the standard theory of the impurity states [3], with the spatial structure of the states being reproduced by properly taking into account the *fork* effect.

The first work on the theory of a single magnetic impurity in a conventional *s*-wave superconductor was done by Yu Lu and Shiba [6]. They showed the existence of the intragap states for sufficiently strong magnetic coupling J between impurity spin and conduction electrons. After realization that high- T_c materials are *d*-wave superconductors, the interest in this problem led a number of authors to consider the effect of a single magnetic or nonmagnetic impurity in the *d*-wave case [7,3]. It was argued that impurity scattering will lead to the highly anisotropic response in the density of states that can be measured by STM [7]. Strong impurity scattering, as opposed to the weak Born scattering case, was shown to introduce the intragap states similar to Yu Lu-Shiba states in the *s*-wave case [3]. With simultaneous advances in STM techniques, Yazdani *et al.* were able to tunnel into magnetic impurity states in Nb thus proving that tunneling into impurity states in *s*-wave superconductors is possible [8]. In more recent STM experiments by Davis *et al.*, impurity states induced by Zn and Ni substitution were observed in optimally doped BSCCO [1].

The starting point of our model is a two-dimensional mean-field (MF) Hamiltonian with the nearest neighbor attraction, V , which yields *d*-wave superconductivity in a range of dopings close to half-filling,

$$H_0 = - \sum_{i,j,\sigma} t_{ij} c_{i\sigma}^\dagger c_{j\sigma} + \sum_{\langle ij \rangle} c_{i\downarrow} c_{j\uparrow} \Delta_{ij}^* + \text{h.c.} \quad (2)$$

Here, $\Delta_{ij} = V \langle c_{i\downarrow} c_{j\uparrow} \rangle$ is the self-consistent MF superconducting order parameter. The hopping t_{ij} equals t for nearest neighbors and t' for the second-nearest neighbor sites i and j . The parameters that are relevant for BSCCO are $t = 400$ meV, $t' = 0.3t$. To match the amplitude of the superconducting gap in optimally-doped BSCCO, which is about 40 meV, we choose the attraction $V = -0.525t$. The chemical potential is chosen to yield 16% doping ($\mu = -t$).

The local impurity is introduced into Hamiltonian Eq. (2) by modifying the electron energy on a particular site. The corresponding addition to the Hamiltonian is

$$H_{\text{imp}} = V_{\text{imp}}(n_{0\uparrow} + n_{0\downarrow}) + S_{\text{imp}}(n_{0\uparrow} - n_{0\downarrow}). \quad (3)$$

The first term is the potential part of the impurity energy that couples to the total electronic density on site 0, and

the second term describes the magnetic interaction of the impurity spin and the electronic spin density on the same site. We assume that the impurity spin is large and can be treated classically, as if it were a local magnetic field. Our goal is to determine V_{imp} and S_{imp} so as to match both the location of the impurity states within the gap and the spatial distribution of their intensity.

We solve the MF equations self-consistently on a square ($N \times N$) lattice with periodic boundary conditions. The Hamiltonian $H = H_0 + H_{\text{imp}}$ can be rewritten in the matrix form, $H = \mathbf{c}^\dagger \hat{H} \mathbf{c}$, with $\mathbf{c} = (c_{1\uparrow}, c_{1\downarrow}^\dagger, c_{2\uparrow}, c_{2\downarrow}^\dagger, \dots)^T$, where \hat{H} is a $(2N^2) \times (2N^2)$ hermitian matrix and subscripts of c run through all lattice sites. By applying a unitary transformation α the Hamiltonian matrix can be diagonalized as $\hat{H} = \alpha \hat{D} \alpha^{-1}$, with $D_{nm} = \delta_{nm} E_n$. The quasiparticles that diagonalize the Hamiltonian are the Bogoliubov quasiparticles,

$$\gamma_n = \sum_m (\alpha^{-1})_n^m c_m, \quad (4)$$

with energies E_n . The original creation-annihilation operators can be expressed in terms of the Bogoliubov quasiparticles,

$$c_{(i,j)\uparrow} = \sum_n \alpha_{(i,j)\uparrow}^n \gamma_n, \quad (5)$$

$$c_{(i,j)\downarrow}^\dagger = \sum_n \alpha_{(i,j)\downarrow}^n \gamma_n, \quad (6)$$

where we replaced c_m by the explicit form of these operators. From the above expressions it is clear that $\alpha_{(i,j)\uparrow}^n$ corresponds to the amplitude of spin-up wave function with energy E_n on site (i, j) , while $(\alpha_{(i,j)\downarrow}^n)^*$ is the amplitude of the spin-down wave function with energy $(-E_n)$ on the same site. Using these wavefunctions one can recompute the mean-field parameters.

First let us analyze the position of the impurity energy level as a function of the impurity potential. The results are presented in Figure 2. All impurities placed in a superconductor generate quasiparticle weight both on positive and symmetric negative biases. The sign of the energy level is defined based on where the majority of the quasiparticle weight resides. Attractive impurities produce energy levels lying below the Fermi surface, while repulsive ones generate states with positive energy. In the limit of a very strong impurity potential both attractive and repulsive impurities generate identical states with a small residual energy related to the amount of the particle-hole symmetry breaking, caused by the specifics of the band structure and doping [9].

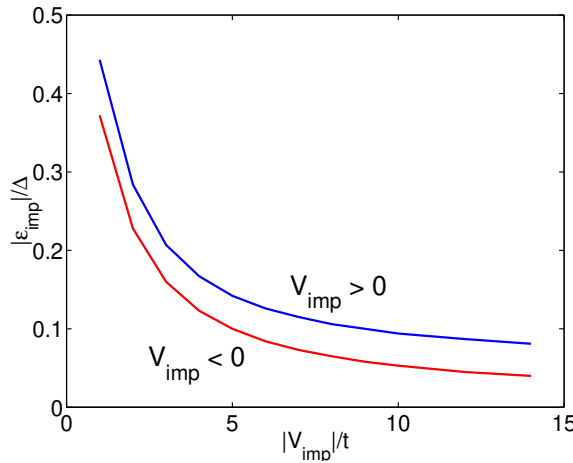


FIG. 2. Impurity energy level position as a function of the potential impurity strength, V_{imp} . The blue (top) line corresponds to repulsive impurities, which produce positive energy levels ($\epsilon_{\text{imp}} > 0$); the red line is for attractive impurities, which generate negative energy states ($\epsilon_{\text{imp}} < 0$). For strong impurity potential both energies converge to the same small value determined by the amount of particle-hole symmetry breaking.

The analysis of the energy level positions implies that the Zn impurity can be associated with a strong attractive potential, $V_{\text{Zn}} = -11t = -4.4$ eV and $\epsilon_{\text{Zn}} = 0.005t = -2$ meV. Ignoring for now the level splitting, the Ni case can be associated with a relatively weak repulsive impurity, $V_{\text{Ni}} = t$ and $\epsilon_{\text{Ni}} = 0.0443t = 18$ meV. These impurity energies are in agreement with the general band structure arguments. Zn^{2+} ion has 10 electrons that completely fill d orbitals. Hence, the $d_{x^2-y^2}$ orbital of Zn, relevant for interaction with Cu-O plane orbitals, is deep below the Fermi surface. On the other hand, Ni has 8 electrons in the d shell, with the $d_{x^2-y^2}$ being unoccupied, but with a small energy, given by the level splitting within the d shell.

The spatial distribution of the spectral intensity corresponding to the Zn impurity is shown in Figure 3. The top two plots show the intensity $A_{i,j}^{\text{CuO}}$ as it would be seen by an STM tip imaging directly Cu-O layer. The intensity is related to impurity state wavefunction Ψ on site (i,j) ,

$$A_{i,j}^{\text{CuO}} = |\Psi_{i,j}|^2. \quad (7)$$

The intensity on the impurity site is strongly suppressed due to the strong impurity potential. The bottom two plots correspond to imaging through the top Bi-O layer. They are obtained by applying a filtering function $F[\Psi] = |M_{i,j}|^2$ to the impurity state wavefunction Ψ . The effect of the filtering function is to produce the intensity

$$A_{i,j}^{\text{BiO}} \propto |\Psi_{i+1,j} + \Psi_{i-1,j} - \Psi_{i,j+1} - \Psi_{i,j-1}|^2. \quad (8)$$

Indeed, the intensity on the Bi-O layer is maximized on the impurity site due to the interference of the contributions from the impurity's nearest neighbor sites.

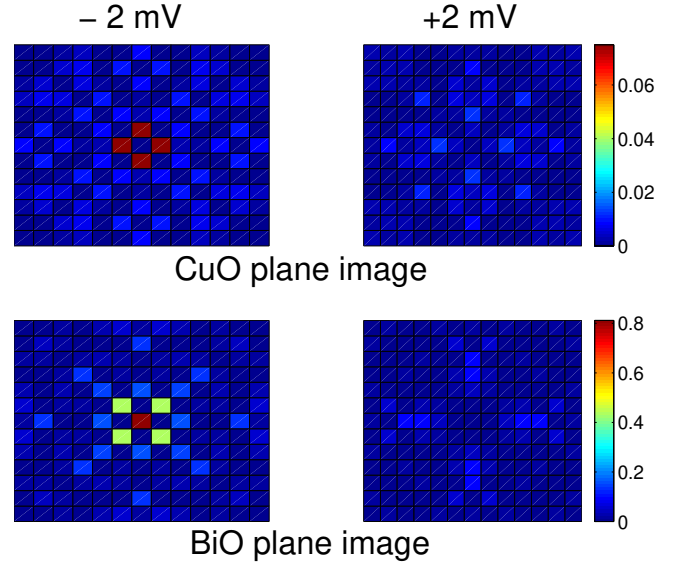


FIG. 3. Top two plots show the real-space intensity of the Zn impurity state in the Cu-O plane. While most of the intensity is concentrated on the negative bias, -2 meV, as it is seen in the experiments [1], the spatial shape of the state does not agree with the experimental results. The bottom two plots show the same impurity state, but as seen through the Bi-O layer. The figure is obtained by applying the filter function of Eq. (1). The energy of the state and the spatial intensity distribution agree with experiment [1].

The form of the filter function of Eq. (1) follows from the analysis of the dominant tunneling channels between the Cu-O and Bi-O layers. An electronic state that resides on the Cu $d_{x^2-y^2}$ orbitals reaches the STM tip by tunneling through overlapping $4s$ orbitals of neighboring Cu and $4s$ orbitals of Bi (Figure 1). The substitution of Cu by Zn or Ni does not affect this channel. Therefore, tunneling into a particular Bi atom on the surface effectively probes four nearest neighbor Cu $d_{x^2-y^2}$ orbitals in the Cu-O plane. The sign of a contribution of an individual orbital is given by the sign of the effective overlap between the orbital and the high-energy $4s$ level through which the tunneling occurs. Here we assume that tunneling between planes occurs predominantly through $4s$ orbitals of Cu, Zn and Bi. This is certainly true for the interlayer tunneling between Cu-O planes in pure materials and has been emphasized by many authors [4,5]. The angular effect of the filter on the far asymptotic of the impurity states was discussed earlier [10]. An alternative explanation and a different form of the filter was considered by Zhu *et al.* [11].

The structure of the Ni state is more complicated than the Zn case. It appears on both positive and negative biases. In addition, there is a peak splitting on each bias. Unlike Zn, Ni impurity is magnetic, with spin 1. To simulate the effect of spin we include a non-zero spin part of the impurity potential, $S_{\text{imp}} \neq 0$, in the Hamiltonian Eq. (3). The spin component introduces level splitting between “up” and “down” spin states. Figure 4a shows the amplitudes of the spin-split states on the impurity sites and its neighbors for $V_{\text{Ni}} = t$ and $S_{\text{Ni}} = 0.4t$. The spin-split energy levels are $\varepsilon_{\downarrow} = 0.0522t$ and $\varepsilon_{\uparrow} = 0.0369t$. The total spin-up and spin-down intensities for each bias are shown in Figure 4b. Both figures (a) and (b) correspond to the image observed through the Bi-O layer. The general shape of the states agrees well with the experimental data [2]. We do not find, however, the approximate equality of the total weights on positive and negative biases observed experimentally. The total weight on the negative bias is about factor of 3 smaller than the weight on the positive bias.

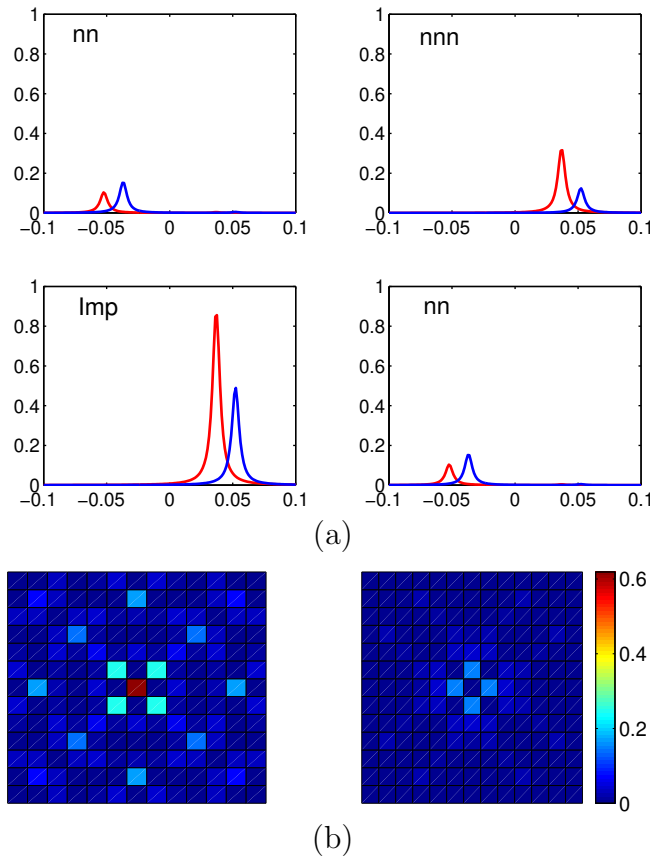


FIG. 4. (a) Spectral intensity on the impurity site, its nearest neighbors (nn), and next nearest neighbor (nnn). Impurity potential is $V_{\text{Ni}} = t$ and $S_{\text{Ni}} = 0.4t$. Red line is spin up, and blue is spin down. (b) Intensity map for the combined spin up and spin down states.

Some aspects of the Ni-impurity state cannot be addressed within the simple framework of our theory. We assumed that the spin of the impurity is static and plays the role of a local magnetic field. Hence, we completely ignored the fluctuations of the Ni spin. There is, however, one experimental aspect where the effects of spin fluctuations may be crucial. In our theory, both Ni and Zn impurities suppress superconductivity in their vicinities. Experimentally, however, only Zn suppresses superconductivity, while Ni doesn't affect the magnitude of the superconducting gap. A possible explanation is that the magnetic character of Ni impurity allows it to participate in the spin fluctuations, which are believed to be the driving mechanism of the high-temperature superconductivity.

In the case of Zn, we focused on the large *local* potential scattering off the impurity as a main effect to account for the STM intensity distribution. It is important to mention that Zn substitution also induces magnetic moment, which can be observed in magnetic susceptibility and NMR measurements [12]. The quenching of magnetic moment around Zn could in principle lead to the Kondo resonance near the Fermi surface, as has been proposed by Polkovnikov *et al.* [13]. This effect however, would require a very strong exchange coupling J to overcome the vanishing of the density of states at low energies, and would be strongly temperature dependent above 20K.

In conclusion, we have demonstrated that recently observed Zn and Ni impurity states in BSCCO [1,2] can be explained by simple model of strong potential impurity in the case of Zn and mixed (potential + spin) impurity in the case of Ni, interacting with a *d*-wave superconducting condensate. The crucial aspect that we have included in the present treatment is the effect of the Cu-O to Bi-O interlayer tunneling.

We are grateful to J.C. Davis, S.H. Pan, S. Sachdev, and M. Vojta for useful discussions. This work has been supported by US DoE.

[1] S. H. Pan, E. W. Hudson, K. M. Lang, H. Eisaki, S. Uchida, and J. C. Davis, *Nature*, **403**, 746-750 (2000)
[2] J. C. Davis, private communication.
[3] A. V. Balatsky, M. I. Salkola, and A. Rosengren, *Phys. Rev. B* **51**, 15547 (1995); A. V. Balatsky and M. I. Salkola, *Phys. Rev. Lett.* **76**, 2386, (1996); M. Salkola, A. V. Balatsky, and J. R. Schrieffer, *Phys. Rev. B* **55**, 12648-12661 (1997).
[4] S. Chakravarty, A. Sudbo, P.W. Anderson, and S. Strong, *Science* **261**, 337 (1993).
[5] O.K. Andersen, A.I. Lichtenstein, O. Jepsen, F. Paulsen, *J. Phys. Chem. Sol.* **56**, 1573 (1995).

- [6] L. Yu, *Acta Physica Sinica* **21**, 75 (1965); H. Shiba, *Prog. Theor. Phys.* **40**, 435 (1968).
- [7] J. M. Byers, M. E. Flatte, and D. J. Scalapino, *Phys. Rev. Lett.* **71**, 3363 (1993).
- [8] Yazdani, A., Jones, B. A., Lutz, C. P., Crommie, M. F. and Eigler, D. M. *Science* **275**, 1767-1770 (1997).
- [9] H.V. Kruis, I. Martin, A.V. Balatsky, preprint cond-mat/0008349 (2000).
- [10] A.V. Balatsky, *Nature*, **403**, 717-718, (2000).
- [11] J.X. Zhu, C.S. Ting, and C.R. Hu, *Phys. Rev. B* **62**, 6027 (2000); J.X. Zhu, C.S. Ting, cond-mat/0012276.
- [12] H. Alloul *et al.*, *Phys. Rev. Lett.* **67**, 3140,(1991); A.V. Mahajan *et al.*, *Europhys. Lett.* **46**, 678, (2000); M-H. Julien *et al.*, *Phys. Rev. Lett.*, **84**, 3422, (2000).
- [13] A. Polkovnikov, S. Sachdev, and M. Voita, cond-mat/0007431.